Bull Mater Sci (2020)43:251
https://doi.org/10.1007/s12034-020-02215-2

Sonochemically synthesized $Na_2Ti_6O_{13}$ nanorod: an efficient electrode material for Na-ion battery

SWATILEKHA GHOSH[1,2]

[1] Faraday Materials Laboratory, Materials Research Centre, Indian Institute of Science, Bangalore 560012, India
[2] *Present Address:* Dr. M. N. Dastur School of Materials Science and Engineering, Indian Institute of Engineering Science and Technology, Shibpur, Howrah 711103, India
slghosh@matsc.iiests.ac.in; yourslekha@gmail.com

MS received 23 February 2020; accepted 4 June 2020

Abstract. A simple cost-effective wet synthesis route has been proposed for synthesis of $Na_2Ti_6O_{13}$, which is an efficient anode material that can be used for 1–3 volt batteries. The material has been synthesized by sonochemical route, which offers two distinct features: (1) energy-savvy (green) synthesis by significantly lowering the final calcination temperature and duration, and (2) formation of uniform and nano-scale particles suitable for battery application. The sonochemical synthesis was carried out at 20 kHz–500 W by applying sonication for 30 min at 25°C, using precursors ($NaOH:TiO_2$) in a molar ratio of 6:1 followed by calcination at 750°C for 1 h in air. This material showed excellent reversible electrochemical performance (up to 93% retention) and offers reversible capacity around 40 mAh g^{-1} acting to be 0.82 V anode for Na-ion battery.

Keywords. Sonochemistry; Na-ion battery; nanorod; anode material; $Na_2Ti_6O_{13}$.

1. Introduction

With the goal of minimizing the safety issues in commercializing rechargeable batteries, implementation of suitable anode materials is mandatory. Carbon-based anodes have been successfully commercialized to meet this issue. In case of Na-ion batteries, hard carbon showed high sodium insertion capacity [1,2]. However, due to the very low intercalation potential, these anodes lead to decomposition of the electrolyte [3]. As an outcome, these materials can instigate various safety concerns during charging procedure. This property of hard carbon has been identified as the biggest drawback in its way of commercialization [4,5].

Seeking alternate materials chemistry, Ti-based anodes were introduced, which can be operated at slightly higher voltage, with high capacity [6–9], long cycling stability [6] and good thermal stability [10]. These types of anode materials are economic, eco-friendly with a full cell operation voltage of 2.5 to 3.5 V when coupled with high voltage cathode materials [11–13]. In this respect, particularly Na–Ti–O-based anode materials showed plateau in the voltage range of 0.4–1 V with capacity ranging from 50 to 200 mAh g^{-1} [14,15]. In the quest for safe anode material, material should be chosen with moderate Na^+ intercalation voltage. For $Na_2Ti_6O_{13}$ (NTO), the Na^+ intercalation voltage was found at 0.8 V where electrochemical equation for Na storage is explored as, $Na_2Ti_6O_{13} + xNa^+ + xe^- = Na_{2+x}Ti_6O_{13}$, $x = 1$ refers to theoretical capacity of 49.5 mAh g^{-1} [10,16]. Additionally, NTO showed excellent cycle life and fast rate kinetics [10,16].

At present, nano-structured materials have shown unique features and properties with respect to traditional bulk materials. Even nano-structured electrode materials have opened a new avenue in the development of energy storage devices. These nano-structure electrodes deliver better capacity and rate kinetics [17–22] when compared to electrode material dimensions in micro or in higher range. This enhanced performance is possible due to increasing surface area of contact between electrode and electrolyte. Previously for suitable electrode application various nano-structured materials such as nano-tube, nano-wire, rod and pillar have been investigated intensely [23–32]. These surface modifications also reduce the diffusion path with the particles, which simplifies Na-ion intercalation immensely [33]. Thus, the strategy to synthesis these high-performance nano-materials are essential [21].

The first report on NTO follows solid-state synthesis involving calcinations for several days [16] and the end product were aggregated several micrometre large particles with impurity from rutile TiO_2. This material delivered only 52% of the theoretical capacity at very low applied current (C/50 rate). To improve this electrochemical performance further nano-structure material were synthesized. Previously, NTO synthesized by soft template method [10] delivered nanorod materials with dimension as 100 × 1000 nm (width × length). This nanorod showed excellent

Published online: 02 September 2020

retention property offering reversible capacity of 80% of the theoretical capacity. The NTO prepared by solution-combustion method [14] also showed similar electrochemical properties. Even NTO thin films in the nano-range obtained by pulse laser deposition technique have shown excellent results for Na-ion micro battery system [34]. These synthesis processes involve various high purity, pricey and exclusive precursors and later calcination at high temperature for longer duration. In few cases the synthesis process turned to be a costly and energy demanding by fabrication involving expensive and sophisticated technique. Thus, there is a need to synthesis nano-scale materials *via* economic and ecofriendly route.

This article focuses on synthesis of nano-structure NTO material by an energy-savvy route in general and sonochemical synthesis in particular. The special features of the sonochemical synthesis is (1) formation of uniform and nano-scale particles from easily available and economic hydroxide and oxide precursors and (2) energy-savvy (green) synthesis by significantly restricting the final calcination temperature and duration. The detailed studies reported herein reveal the excellent Na-ion diffusion during cycling process, delivers up to 80% of the theoretical capacity with a 93% of capacity retention.

2. Experimental

2.1 *Materials*

The precursors NaOH (SD Fine-Chem Limited) and TiO_2 (anatase, Merck) were used for this synthesis, irrespective of dry or wet method. The ethanol used in the wet method was obtained from Jiangsu Huaxi International. The NaOH pellets and TiO_2 powder were used for all type of experiments. These precursors are economic and easily available in the market. Reagent grade (purity ≥97%) chemicals were used for all experiments. Any further purification was not carried before experimentation.

2.2 *Synthesis*

To explore the possibility of economic and energy miser preparation of $Na_2Ti_6O_{13}$, two types of synthesis method have been carried out, such as dry and wet methods. The dry synthesis was carried out *via* dry mixing method, i.e. planetary ball milling using micro ballmill P7. Here the precursors NaOH and TiO_2 were mixed in molar stoichiometry of 1:3, respectively. This mixing was carried out in a stainless steel container (250 ml) using 13 stainless steel balls at 400 rpm for 4 h to obtain 2.5 g mixture. This mixture was calcined at 750°C for 2 h to achieve the final product.

For wet synthesis process, sonochemical reaction route was chosen. Sonication was carried out in Sonics & Materials VCX 500 sonifier (500 W with amplitude of 35%, 20 kHz), operated by Ti probe (ϕ = 13 mm) was immersed inside the mixture of alcohol and hydroxide-TiO_2 salts. The sonicated products were obtained by applying the irradiation for 30 min at 25°C followed by an alcohol wash and drying in air at 60°C for 12 h. Finally, this dry powder was calcined at 750°C for 1 h in air to complete the synthesis process.

The choice of precursor ratio and their proportion with the solvent went through several trials. For trail, precursor proportion was chosen in the molar ratio (NaOH:TiO_2) range of 1:1 to 6:1. The successful synthesis was identified as molar ratio of NaOH:TiO_2 as 6:1, when 2.44 g:0.807 g was added in 40 ml of ethyl alcohol, respectively. It was difficult to determine the suitable ratio of NaOH:TiO_2: ethanol due to their solubility limit. As NaOH is more soluble in ethanol with respect to TiO_2 nano-particles, it was difficult to determine the wt% of NaOH in the solution for sonochemical reaction. In lower concentration of NaOH, obtained product showed high content of TiO_2. As an outcome, the ratio of the precursor and solvent was chosen in such a way that all the precursors will not dissolve fully in the solvent.

The reaction between these precursors when ultrasonic wave was applied to them can be explained in terms of primary and secondary reactions. These primary and secondary reactions take place during the bubble collapse at its centre and periphery, respectively, from acoustic cavitation. During primary reaction, $O^{\bullet}$ and $OH^{\bullet}$ radicals might form inside the bubble from sonolysis of alcohol. The synthesis of metal oxide using non-volatile precursors in volatile solvent follows a secondary sonochemistry. The formation of radicals in the hot spot leads to further reaction with the metal ions present in the solvent. It is explained previously [35] that sonochemical synthesis of metal oxides involving non-volatile precursors in a volatile solvent follows secondary sonochemistry by formation of oxygen radical ($O^{\bullet}$) from the ultrasonic irradiation of ethanol. The overall sequential implicit reactions for redox chemistry in this system are given below:

$$C_2H_6O \rightarrow O^{\bullet} + 2CH_3^- \quad (1)$$

$$NaOH \rightarrow Na^+ + OH^- \quad (2)$$

$$TiO_2 \rightarrow TiO + O^{\bullet} \quad (3)$$

$$2TiO_2 \rightarrow Ti_2O_3 + O^{\bullet} \quad (4)$$

$$2Na^+ + O^{\bullet} \rightarrow Na_2O \quad (5)$$

$$Na_2O + 3Ti_2O_3 + 3O^{\bullet} \rightarrow Na_2Ti_6O_{13} \quad (6)$$

2.3 *Structural and physical characterization*

To determine the crystalline structure and purity of the samples, PAN analytical X'Pert Pro diffractometer [Cu-Kα source (λ_1 = 1.5408 Å, λ_2 = 1.5443 Å)] operating at

40 kV/30 mA was used. To obtain these diffraction patterns, the 2θ range was maintained from 10 to 65° (step size of 0.026° s^{-1}) in each case. The obtained crystalline structure was further illustrated using the VESTA software. Synchrotron X-ray diffraction patterns were collected at the BL-18B Indian beam line (High Energy Accelerator Research Organization, KEK-Photon Factory, Tsukuba, Japan). Energy of beam line (E = 15.77 keV) was calibrated with Si (640b NIST) standard and the wavelength (λ) was calibrated to be 0.786 Å. Again purity estimation was achievable by Rietveld refinement measurement, which was carried out by GSAS software program. FEI Inspect F50 scanning electron microscopy (10 kV) and FEI Tecnai F30 S-Twin transmission electron microscope (TEM, 200 kV) were used to inspect the morphology. TEM sample was prepared by dispersing the powder sample in acetone and later few drops of the acetone solution was drop-casted on a copper grid.

2.4 *Electrochemical characterization*

The electrochemical experiment was performed by assembling home-made Swagelok type PTFE cells using sodium metal foil (S.D. Fine Chem. Ltd) as counter cum-reference electrode. An absorbent glass matrix (thickness = 1.15 mm) was used as a separator. To fabricate the working electrode, the active material (80 wt%), acetylene black (Alfa Aesar, 10 wt%) and polyvinylidene fluoride (Aldrich, 10 wt%) were mixed together. Then few drops of n-methylpyrrolidone (Aldrich) was also added to this ground material to produce the slurry. Finally, slurry was casted on pre-treated copper foil (thickness = 0.10 mm) to achieve the loading weight of active material around ~2–3 mg cm^{-2} followed by vacuum dry at 100°C for 12 h. As a part of pretreatment process, the Cu foils were initially degreased using detergent and soap water followed by an etching procedure in 3 M HCl for 30 s and then vacuum dry at 40°C. Finally, the half cells were fabricated into Ar-filled glove box (MBraun model UNILAB, GmbH, Germany) maintained at moisture and oxygen content levels below 1 ppm. In these half cells, 1 M $NaPF_6$ solution in propylene carbonate was used as the electrolyte. The measurement was carried out using ~3 mg active material. Cyclic voltammetry and charge–discharge cycling were carried out in Bio-Logic (Claix, France) VMP3 potentiostat/galvanostat battery test cycler. These half cells were galvanostatically cycled in the voltage range from 0.5 to 2.5 V applying various current densities at room temperature.

3. Results and discussion

Figure 1 shows the powder XRD pattern of the materials synthesized by sonochemical method by taking various ratios of the precursors NaOH:TiO_2. The XRD pattern of all sets matches with standard powder diffraction pattern of $Na_2Ti_6O_{13}$ (JCPDS card no. #73-1398). However, few prominent peaks from TiO_2 precursor are noticeable. These

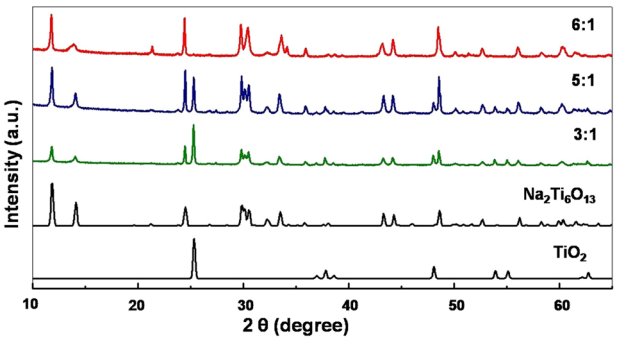

Figure 1. Comparative XRD pattern of nano-materials prepared by sonochemical method by varying the precursor ratio of NaOH:TiO_2, calcinations at 750°C for 1 h.

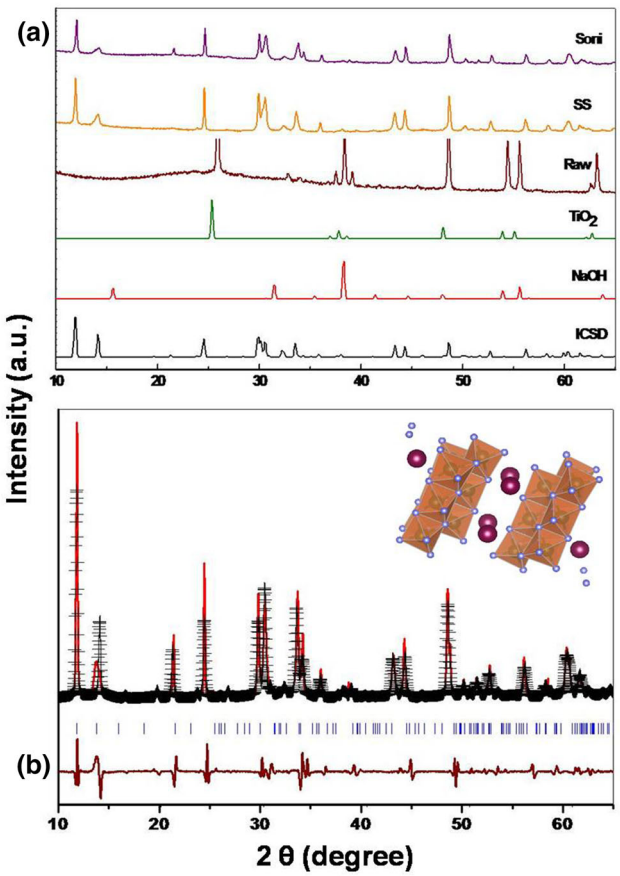

Figure 2. (**a**) Comparative XRD pattern of nano-materials prepared by dry and wet methods, Soni: sonochemically synthesized followed by calcinations at 750°C for 1 h, SS: mechanical ball milling followed by calcinations at 750°C for 2 h; (**b**) Rietvelt refinement of synchrotron patterns of nano-materials prepared by sonochemical reaction followed by calcination for 1 h at 750°C. (Inset) Illustration of the crystal structure of $Na_2Ti_6O_{13}$.

peaks disappeared when the precursor ratio was tuned to 6:1.

Figure 2a shows the powder XRD pattern of the materials synthesized by dry and wet methods, before and after calcination. Here the optimized product from the wet method has been presented for comparison. The XRD pattern of the synthesized materials matches perfectly with standard powder diffraction pattern of $Na_2Ti_6O_{13}$ (JCPDS card no. #73-1398) irrespective of synthesis method, which is a monoclinic structure that belong to space group C2/m. Thus, phase pure material synthesis is possible from both methods involving shorter annealing duration in comparatively lower temperature. The XRD pattern of the sonicated raw powder matched mostly the pattern of precursor TiO_2 with very few peaks of NaOH. It is prominent that due to sonochemical reaction TiO_2 precursor has been modified with little presence of NaOH. After calcination any peaks from the precursors was not found. The phase purity of the calcined material was verified with reitveld refinement analysis, which was carried out with the pattern obtained from synchrotron XRD study, as shown in figure 2b. Figure 2b shows the experimental data points by black cross, simulated pattern by red line, their difference by brown line, and Bragg diffraction positions by blue tick marks. The pattern showed a good match with $CHI^2 = 25\%$ and the details on the lattice and other parameter are shown in table 1. These values showed good match with the values reported earlier [10,14].

The structure of $Na_2Ti_6O_{13}$ is based on distorted octahedron, where each Ti-ion is associated with six oxygen ions at the corners. At one level, these octahedra shares edges in a linear group of three, followed by joining with the group above and below it forming a zigzag ribbon-like structure, as shown in figure 2b. This arrangement of hexatitanate provides tunnel for Na intercalation in open octahedral framework along the *b*-axis.

Figure 3 shows the SEM image of the sonochemically synthesized nano-materials before and after calcinations, indicating uniform distribution of nano-materials with particles of spherical structure. Sonochemical reaction delivers uniform-spherical-nano-scale materials, as shown in figure 3a. The particle size of these obtained sonicated product were found to be around 100 nm. Figure 3b illustrates the morphology of the sonicated products after calcinations. The uniform distribution of nano-materials is retained after calcinations with particles of rod-like structure. This uniform and homogeneous distribution of nanorods with the particle size of 80–100 nm in diameter and 300–200 nm in length is beneficial for electrochemical measurements. The TEM image of these nanorods are shown in figure 3c, the particle size obtained from TEM analysis confirms the SEM analysis. Previously, nanorods have been prepared by solution-combustion [14] and soft-template methods [10], these have similar morphology as reported in this article. This nano-scale morphology accelerates Na-ion diffusion effecting excellent electrochemical performance. On the other hand, the nanorods obtained from mechanical ball milling (solid-state synthesis) at 400 rpm for 4 h followed by calcination at 750°C for 2 h showed larger particles (300 × 1000 nm) compared to sonochemical synthesis, as shown in figure 3d. It is important to note that the reduction in the final calcination temperature and duration influences the particle size and a nano-structure is obtained by restriction in unwanted grain growth and coarsening. However, the solid-state synthesis gives larger particle size which might be an outcome of the long mixing process with respect to sonochemical reaction. Earlier similar results were seen for solid-state synthesis *vs.* sonochemical synthesis designed for $Na_2Li_2Ti_6O_{14}$ [36]. The morphology obtained from solid-state method showed larger particles in the range of several micrometres, reported earlier too [16].

Standard Na-half cell architecture has been used for studying electrochemical performance of this material. The electrochemical study was carried out with the sonochemically synthesized product only due to its nano-size morphology, which is 3 times smaller with respect to dry synthesis method. Figure 4a shows the potential for redox activity with variation in cycle number. For 1st cycle, this potential value is found as 0.9 V, determined from the flat plateau region of figure 4a. In the 2nd cycle, this potential value decreases to 0.85 V and this value remains constant up to 50th cycle. Similar potential value for redox activity has been reported previously [10,14,16]. The discharge capacity value is determined as 110 mAh g^{-1} for 1st cycle, shown in voltage-capacity profile of figure 4a. This value is almost two times higher than the theoretical capacity (theo. cap. = 49.5 mAh g^{-1} for 1 Na exchange). In 2nd cycle, this discharge capacity value decreases to 50 mAh g^{-1}. Earlier it is reported as discharge capacity around 50–65 mAh g^{-1} for insertion of 0.96–0.9 Na^+ in case of 1st cycle [10,14]. The capacity value retains about 93% of the 3rd cycle for next 47 cycles, shown in figure 4b. The capacity decrease in the first two cycles might be due to solid electrolyte interface formation, which leads to irreversible capacity loss. After

Table 1. Lattice and other parameters obtained from reitveld refinement analysis.

Lattice parameters	Atoms	Atom coordinates			O_{cc}
		x	*y*	*z*	
a = 15.13 Å	Ti1	0.07914	0.00000	0.43348	1
b = 3.74 Å	Ti2	0.17554	0.00000	0.74531	1
c = 9.19 Å	Ti3	0.39160	0.00000	1.10764	1
$\alpha = 90.00°$	Na	0.52061	0.00000	0.26098	1
$\beta = 99.37°$	O1	0.00000	0.00000	0.00000	1
$\gamma = 90.00°$	O2	0.20748	0.00000	0.22555	1
	O3	0.22012	0.00000	0.21870	1
	O4	0.39298	0.00000	0.49397	1
	O5	0.25135	0.00000	0.52872	1
	O6	0.32897	0.00000	0.82627	1
	O7	0.14221	0.00000	0.98786	1

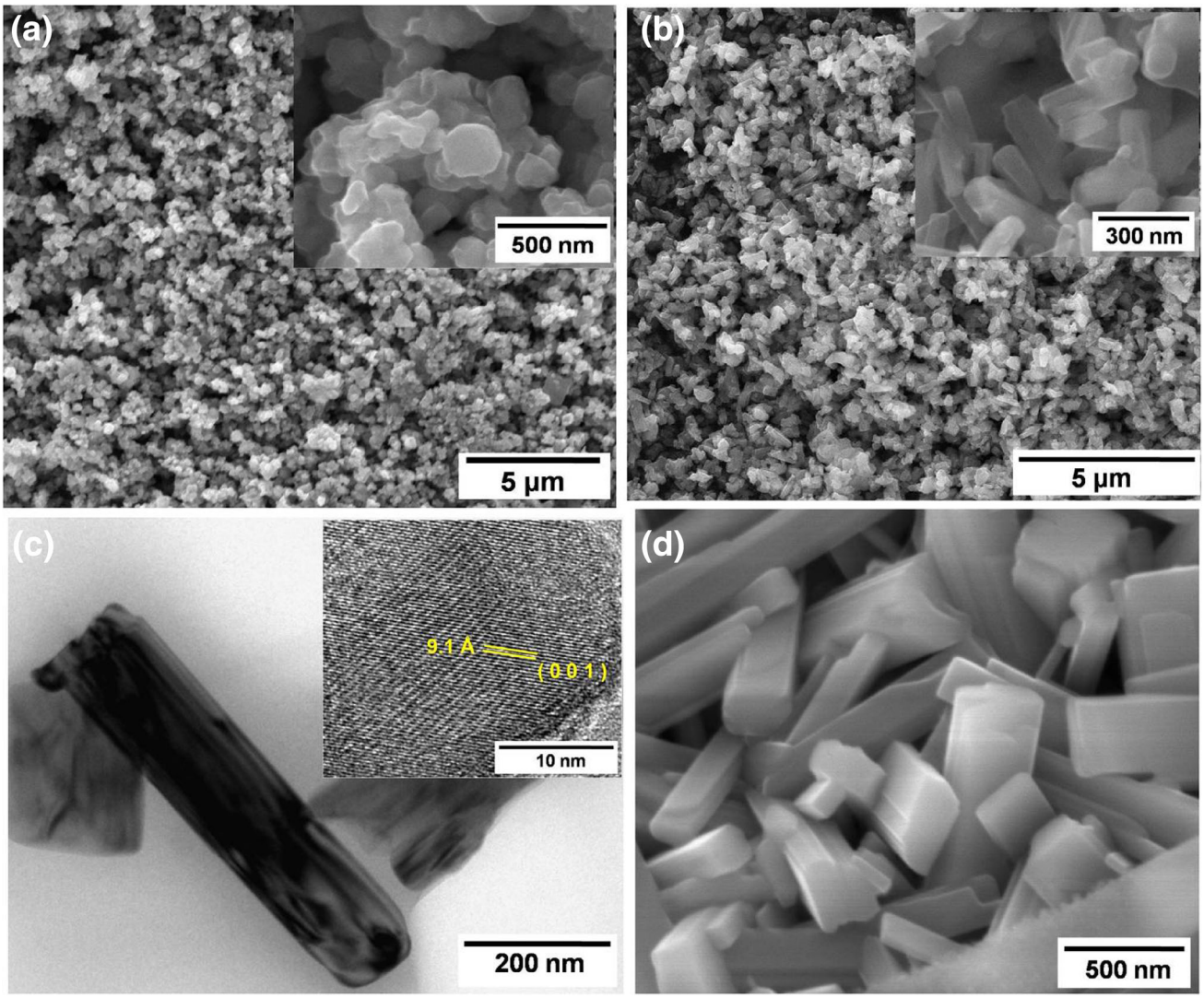

Figure 3. (**a**) SEM micrograph of $Na_2Ti_6O_{13}$ prepared by sonochemical synthesis before calcination. (**b**) SEM micrograph after calcining at 750°C for 1 h. (Inset) Close view of the particle distribution. (**c**) TEM image of a single nano-particle (synthesized sonochemically) with dimension confirming the values from SEM measurement. (Inset) Atomic planes of the nano-particles shown by HRTEM. (**d**) SEM micrograph of $Na_2Ti_6O_{13}$ prepared by solid-state method.

first two cycles, around 0.75 Na^+ insertion takes place in the subsequent cycles, this value matches well with literature value [10,14]. The coulombic efficiency was found around 95% for all cycles, shown in figure 4b. Figure 4c shows the rate kinetics when cycled between C/20 and 2C rates, which indicates good capacity retention property. It also demonstrates the cyclic stability after the rate test, profile indicates that the capacity bounce back near to 40 mAh g^{-1} when tested at C/20 rate. With variation in cycling rate any change in potential for redox activity was not observed. The capacity retention value for various cycling rates is determined as 92, 81, 70, 58 and 45% in C/10, C/5, C/2, C and 2C rate, respectively, with comparison to C/20 rate. Finally after examining for higher rate kinetics, C/20 rate was employed at the end and capacity retention was 95%. Owing to the nano-structure material the Na-ion diffusion has been enhanced, which helped in improvement of rate kinetics. Previously similar result was found for rate kinetics when nano-structure materials were achieved *via* solution combustion method [14]. The retention property at higher rate can be further improved by addition of CB conductive additives or graphite, which opens an extra site of Na ion and helps in better electrolyte interaction [10]. The differential galvanostatic profiles (dQ/dV) are showing (figure 4d) single distinctive peak (0.8 V *vs.* Na/Na^+) for first and subsequent discharging/charging process. This single distinctive peak indicates reversible structural transformation during Na-ion exchange for various discharging/charging processes. Moreover, this slopping voltage curve indicates minimal volume change for single-phase homogeneous reaction mechanism.

The cyclic voltammetry measurement was carried out to analyse the electrochemical redox behaviour of sonochemically synthesized $Na_2Ti_6O_{13}$ upon Na-ion insertion and

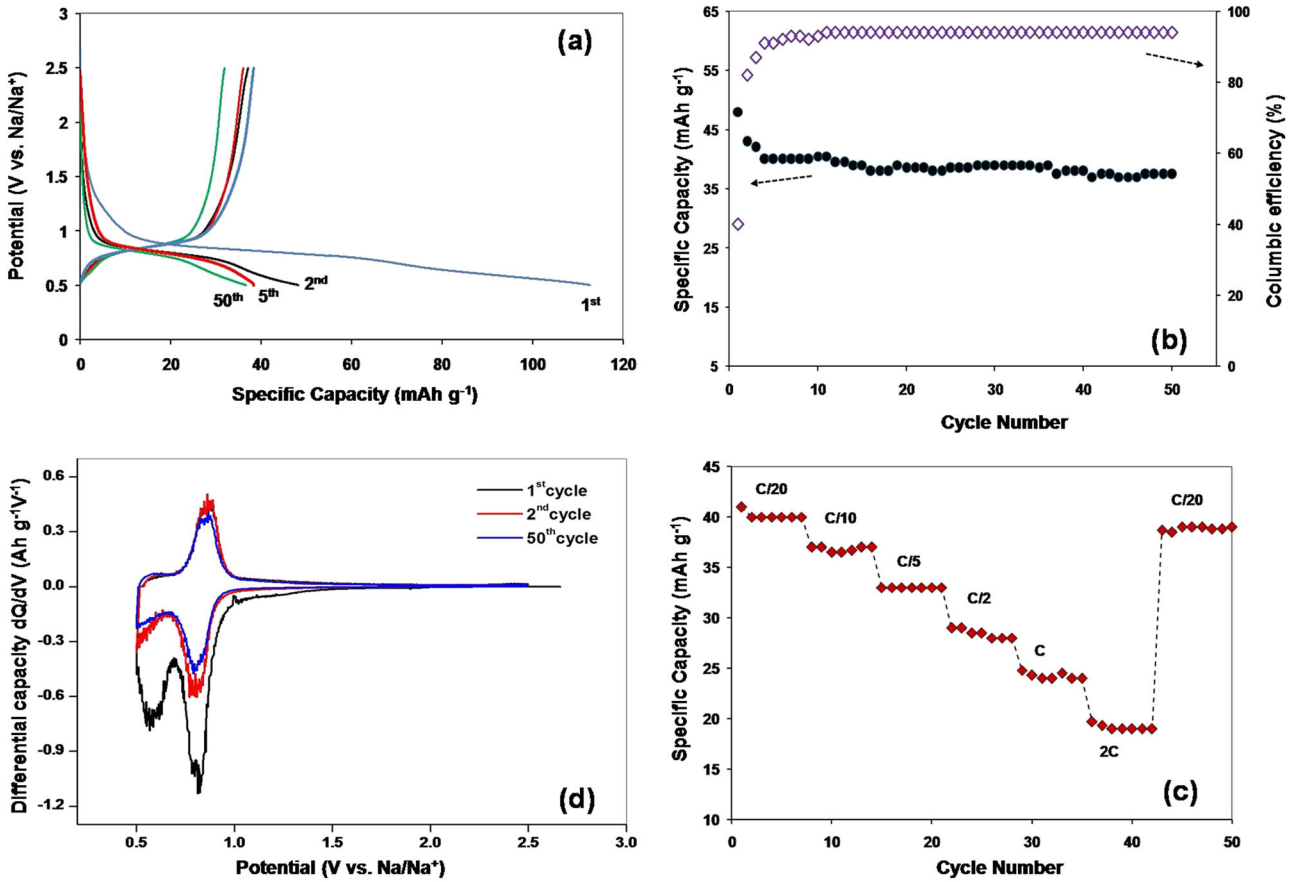

Figure 4. Galvanostatic electrochemical performance of $Na_2Ti_6O_{13}$ anode prepared by sonochemical synthesis calcined at 750°C for 1 h: (**a**) galvanostatic charge–discharge profiles at the rate of C/20, (**b**) cycling stability and coulombic efficiency over a period of 50 cycles at the rate of C/20, (**c**) various rate kinetics at C/10, C/5, C/2, C and 2C and (**d**) the differential galvanostatic profiles (dQ/dV) of $Na_2Ti_6O_{14}$ anode showing two distinctive peaks for all charging/discharging processes.

extraction, as shown in figure 5. The voltammogram was obtained at 0.5–2.5 V potential range, scan rate 0.1 mV s^{-1} shows a single cathodic and anodic sweeps for all cycles. The broad reduction peak was observed at the potential of 0.74 V, indicating only one Na-ion insertion site in the structure. Moreover, in the anodic part one broad peak was observed, which shows a good agreement with the cathodic part.

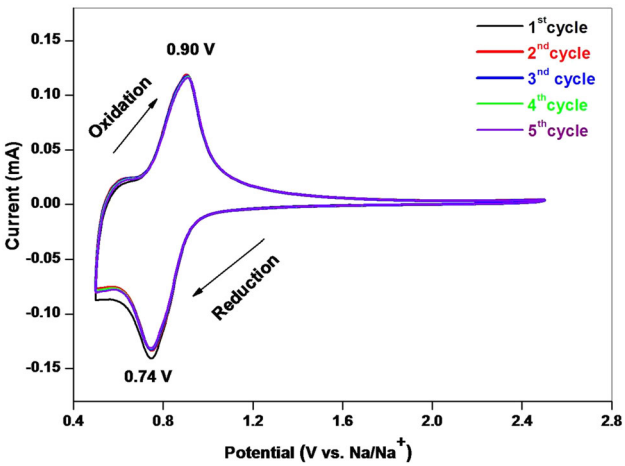

Figure 5. Cyclic voltammograms of $Na_2Ti_6O_{13}$ electrode prepared by sonochemical synthesis calcined at 750°C for 1 h between 0.5 and 2.5 V at a scan rate of 0.1 mV s^{-1}, where Na metal acts as both counter and reference electrodes.

3.1 *General discussions*

(a) At present, the energy storage sector is suffering from economic and energy constraints regarding fabrication of battery materials. Thus, an energy miser preparation route of battery materials is important. In recent years, NTO has been prepared by various methods such as hydrothermal method [37–39], mixing the precursor in agate mortar [40], heat treatment using autoclave [41] and even involving

sonochemical method [42]. The hydrothermal method and autoclave heating process involve heat treatment in lower temperature for several hours in the initial stage, followed by annealing at higher temperature for shorter duration. Other synthesis process involves only annealing at high temperature for several hours. Earlier the sonochemical method reported also has used higher annealing temperature with respect to the annealing temperature reported in this study. Moreover, most of these synthesis methods involve titanium isopropoxide as a precursor, which is very expensive compared to titanium dioxide powder. Thus these previous synthesis routes suggest high purity, pricey and exclusive precursors and later calcination at high temperature for longer duration recommend a synthesis route which is not suitable for large-scale production. This present sonochemical synthesis route suggests calcination at 750°C for 1 h only, involving very economic and easily available precursors. Additionally, this synthesis method can produce 3 g of material involving 40 ml ethanol during sonochemical reaction and it is expected that similar proportionate may be utilized for the large-scale production. Thus this synthesis route can be adopted for industrial production of battery material.

(b) The sonochemical reaction progress *via* acoustic cavitation, which means formation, growth and collapse of bubbles in the liquid media. The massive local temperature, pressure followed by the extra-ordinary heating and cooling generated from the bubble collapse cause high energy chemistry. This kind of chemistry helps in intimate precursor mixing followed by a partial reaction in between from the localized temperature and pressure forming cavities and finally producing nano-scale morphology [36]. This rapid synthesis might produce a NaOH-coated TiO_2, as the sonicated raw product shows a mixed crystalline phase indicating phases of both the precursors. Additionally, the shorter duration of annealing helps in retaining this morphology of the final product. This synthesis route also suggests production of homogeneous nanorod morphology involving smaller Na^+ diffusion length. This obtained nano-scale morphology is suitable for achieving high capacity and retention value. Thus, to attain efficient electrochemical activity in electrodes this synthesis method would be valuable.

(c) The synthesis of phase pure NTO by dry synthesis method is only possible when calcinations were carried out at 750°C for 2 h or above. The decrease in calcination duration indicated a big impurity of the precursor material. Thus, the electrochemical performance of this material might show additional plateaus in the charge–discharge profiles as indicated earlier in the case of $Na_2Li_2Ti_6O_{14}$ [36].

4. Conclusion

The Na–Ti–O-based anode materials were successfully synthesized by sonochemical reaction method from various easily available and economic precursors. Successful synthesis was accomplished by calcination at 750°C for 1 h, resulting in the formation of uniform nanorod particles. The as-synthesized product was found to be an efficient host for reversible Na-insertion, leading to capacity around 40 mAh g^{-1} (at 0.82 V *vs.* Na).

Acknowledgements

Author is grateful to Shanmugha Sundaram Duraisamy and Nookala Munichandraiah from Department of Inorganic and Physical Chemistry, IISc Bangalore, and Prabeer Barpanda from Materials Research Centre, IISc Bangalore, for the immense discussion and technical assistance with electrochemical characterization. Thanks to University Grant Commission (UGC) and Department of Science and Technology (DST), Government of India, for funding this study.

References

[1] Stevens D A and Dahn J R 2000 *J. Electrochem. Soc.* **147** 1271
[2] Stevens D A and Dahn J R 2001 *J. Electrochem. Soc.* **148** A803
[3] Prosini P P, Mancini R, Petrucci L, Contini V and Villano P 2001 *Solid State Ion.* **144** 185
[4] Ge P and Fouletier M 1988 *Solid State Ion.* **30** 1172
[5] Ponrouch A, Marchante M, Courty E, Tarascon J M and Palacín M R 2012 *Energy Environ. Sci.* **5** 8572
[6] Rudola A, Saravanan K, Mason C W and Balaya P 2013 *J. Mater. Chem. A* **1** 2653
[7] Senguttuvan P, Rousse G, Seznec V, Tarascon J-M and Palacin M R 2011 *Chem. Mater.* **23** 4109
[8] Xiao L, Cao Y, Xiao J, Wang W, Kovarik L, Nie Z *et al* 2012 *Chem. Commun.* **48** 3321
[9] Xiong H, Slater M D, Balasubramanian M, Johnson C S and Rajh T 2011 *J. Phys. Chem. Lett.* **2** 2560
[10] Rudola A, Saravanan K, Devaraj S, Gong H and Balaya P 2013 *Chem. Commun.* **49** 7451
[11] Peramunage D and Abraham K M 1998 *J. Electrochem. Soc.* **145** 2609
[12] Jansen N, Kahaian A J, Kepler K D, Nelson P A, Amine K, Dees D W *et al* 1999 *J. Power Sources* **81/82** 901
[13] Ohzuku T, Ueda A, Yamamoto N and Iwakoshi Y 1995 *J. Power Sources* **54** 99
[14] Ghosh S, Daya Mani A, Kishore B, Munichandraiah N, Rao R P, Wong L L *et al* 2017 *J. Electrochem. Soc.* **164** A1881
[15] Zhu G-N, Wang Y-G and Xia Y-Y 2012 *Energy Environ. Sci.* **5** 6652
[16] Trinh N D, Crosnier O, Schougaard S B and Brousse T 2011 *ECS Trans.* **35** 91
[17] Baughman H, Zakhidov A A and de Heer W A 2002 *Science* **297** 787
[18] Sugimoto W, Iwata H, Yasunaga Y, Murakami Y and Takasu Y 2003 *Angew. Chem. Int. Ed.* **42** 4092
[19] Li D L, Zhou H S and Honma I 2004 *Nat. Mater.* **3** 65

[20] Hughes M, Shaffer M, Renouf N C, Singh C, Chen G Z, Fray D J *et al* 2002 *Adv. Mater.* **14** 382
[21] Raimondi F, Scherer G G, Kötz R and Wokaun A 2005 *Angew. Chem. Int. Ed.* **44** 2190
[22] Dong W, Rollison D R and Dunn B 2000 *Electrochem. Solid State Lett.* **3** 457
[23] Wang Y, Lee J Y and Deivaraj T C 2004 *J. Phys. Chem.* **B10** 13589
[24] Wang Y, Lee J Y and Zeng H C 2005 *Chem. Mater.* **17** 3899
[25] Wang Y, Zeng H C and Lee J Y 2006 *Adv. Mater.* **18** 645
[26] Zhao Z W, Guo Z P, Wexler D, Ma Z F, Wu Z and Liu H K 2007 *Electrochem. Commun*. **9** 697
[27] Armstrong G, Armstrong A R, Canales J and Bruce P G. 2006 *Electrochem. Solid State Lett.* **9** A139
[28] Gao X P, Lan Y, Zhu H Y, Liu J W, Ge Y P, Wu F *et al* 2005 *Electrochem. Solid State Lett.* **8** A26
[29] Wang Q, Wen Z and Li J 2006 *Inorg. Chem.* **45** 6944
[30] Armstrong A R, Armstrong G, Canales J and Bruce P G 2004 *Angew. Chem. Int. Ed.* **43** 2286
[31] Hu Y-S, Kienle L, Guo Y-G and Maier J 2006 *Adv. Mater.* **18** 1421
[32] Armstrong A R, Armstrong G, Canales J, Garcia R and Bruce P G 2005 *Adv. Mater.* **17** 862
[33] Lee Y, Kim M G and Cho J 2008 *Nano Lett.* **8** 957
[34] Rambabu A, Senthilkumar B, Sada K, Krupanidhi S B and Barpanda P 2018 *J. Colloid Interf. Sci.* **514** 117
[35] Xu H, Zeiger B W and Suslick K S 2013 *Chem. Soc. Rev.* **42** 2555
[36] Ghosh S, Kee Y, Okada S and Barpanda P 2015 *J. Power Sources* **296** 276
[37] Zhang Y, Hou H, Yang X, Chen J, Jing M, Wu Z *et al* 2016 *J. Power Sources* **305** 200
[38] Cech O, Castkova K, Chladil L, Dohnal P, Cudek P, Libich J *et al* 2017 *J. Energy Storage* **14** 391
[39] Wu C, Hua W, Zhang Z, Zhong B, Yang Z, Feng G *et al* 2018 *Adv. Sci.* **5** 1800519
[40] Ho C K, Vanessa Li C Y and Chan K Y 2016 *Ind. Eng. Chem. Res.* **55** 10065
[41] Luo L, Zhen Y, Lu Y, Zhou K, Huang J, Huang Z *et al* 2020 *Nanoscale* **12** 230
[42] Fagundes N G, Nobre F X, Basilio L A L, Melo A D, Bandeira B, Sales J C C *et al* 2019 *Solid State Sci.* **88** 63